PERGAMON

Transportation Research Part C 11 (2003) 1–28

TRANSPORTATION RESEARCH PART C

www.elsevier.com/locate/trc

Multi-destination traffic flow control in automated highway systems

Luis Alvarez [a,*], Roberto Horowitz [b], Charmaine V. Toy [c]

[a] *Instituto de Ingeniería, Universidad Nacional Autónoma de México, 04510 Coyoacán DF, Mexico*
[b] *Department of Mechanical Engineering, University of California at Berkeley, Berkeley, CA 94720, USA*
[c] *DiCon Fiberoptics, Inc., 1689 Regatta Boulevard, 94804 Richmond, CA, USA*

Received 13 October 1999; accepted 8 April 2002

Abstract

Traffic flow control in automated highway systems (AHS) is addressed. A link layer controller for a hierarchical AHS architecture is presented. The controller proposed in this paper stabilizes the vehicular density and flow around predetermined profiles in a stretch of highway using speed and lane changes as control signals. Multiple lane highways in which vehicles have different destinations and types are considered. The control laws are derived from a model based on a principle of vehicle conservation and Lyapunov stability techniques. The implementation requires only local information. Simulation results are presented.

Keywords: Automated highway systems; Traffic control; Velocity control; Multi-destination traffic; Multi-type traffic

1. Introduction

Automated highway systems (AHS) is a concept proposed to increase capacity and safety in surface transportation systems (Varaiya, 1993). One of the AHS architectures used in the California PATH program consists of five hierarchical layers (Varaiya and Shladover, 1991): network, link, coordination, regulation and physical layers (see Fig. 1). The physical and regulation layers are vehicle based and are related to the vehicle's dynamics and its control. The coordination layer controls the execution of maneuvers; it is based on the group of vehicles involved in each maneuver. The link layer is road-side based and is in charge of regulating vehicle flow on stretches of

* Corresponding author. Fax: +52-55-5622-8090.
E-mail addresses: alvar@pumas.iingen.unam.mx (L. Alvarez), horowitz@me.berkeley.edu (R. Horowitz), ctoy@diconfiber.com (C.V. Toy).

0968-090X/02/$ - see front matter
PII: S0968-090X(02)00019-0

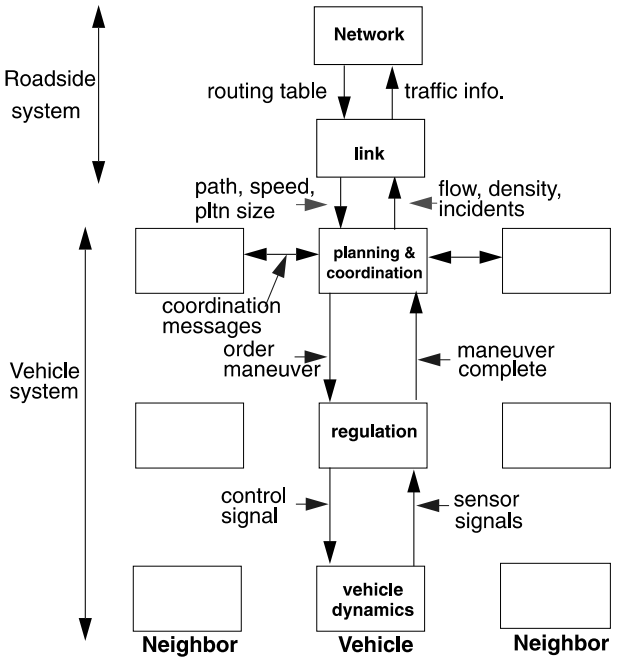

Fig. 1. Hierarchical architecture of AVHS in the PATH program.

highway. Finally, the network layer regulates traffic flow in all the highway network. Readers interested in more detail about the layers of the PATH AHS control architecture are advised to consult, for example (Hsu et al., 1991; Swaroop et al., 1994; Godbole and Lygeros, 1994; Li et al., 1997a,b; Alvarez et al., 1999; Rao and Varaiya, 1994).

The focus of this paper is on control strategies at the macroscopic level of traffic, where the important quantities are the aggregate vehicular density and the traffic flow measured in sections of highway. Some of the relevant control strategies in the literature are reviewed here.

In Karaaslan et al. (1990), the authors present a traffic flow model based on the behavior of human drivers. They replace one of the terms in the model that describe drivers' behavior with a feedback control term designed to homogenize the density. Chien et al. (1993) extend this problem to the tracking of an arbitrary density profile. Using also a macroscopic traffic model based on human driver behavior, they derive a controller that commands a desired velocity at each section of the highway in such way that the density of the entire highway conforms to a specified density profile. The developed control law is based upon the inversion of traffic flow dynamics which becomes difficult when the density in any section is small.

In Rao and Varaiya (1994) a link layer controller consistent with the AHS architecture in Varaiya (1993) is described. The design assumes a fully automated highway and uses a dynamic model of the coordination and regulation layers obtained through extensive simulations under normal operating conditions. In order of priority, lane change proportions, desired speeds and maximum platoon size are possible control variables, although the only control law implemented in SmartPath (Eskafi et al., 1992) is the lane change. The control law is heuristic and therefore does not deal with stability issues.

In Papageorgiou et al. (1990) the goal is to stabilize the traffic flow in the Southern Boulevard Peripherique of Paris. Using only on-ramp metering control, the authors try to achieve a density and flow that is not otherwise possible due to drivers behavior and congestion. Metering control is based on linear quadratic control techniques applied to a linearized traffic flow model that employs only local traffic information. Simulations show that with the on-ramp feedback control congestion is significantly decreased.

In a previous work (Li et al., 1997a,b) a link layer controller for AHS whose goal is to regulate vehicle flow and density in a stretch of highway around desired vehicle density and velocity profiles is presented. It is assumed that for each conceivable scenario (e.g. normal traffic condition, stopped vehicle on highway, blocked or closed lane), a desired behavior of the highway consistent with its capacity under that circumstance can be prescribed. Three topologies are investigated: a single lane highway, a discrete lane highway and a dense lane highway. The $\mathscr{L}_2$ stability of the density error along the stretch of highway is proved when the desired velocities and rates of lane change are time independent. The structure of the proposed control laws is distributed and simple to compute in real time. In Alvarez et al. (1999) the link layer controller presented in Li et al. (1997a,b) is extended to multi-destination and multi-type traffic flow. Lane change commands are treated differently making it possible to control the lane change between lanes with different nominal velocities.

This paper deals with traffic flow stabilization in discrete lane highway topologies. The goal is to regulate aggregate traffic conditions around desired traffic flow profiles in stretches of highway, while acting within the link layer of the PATH AHS hierarchical architecture. To achieve this goal of stabilization, a controller is designed that uses speed and lane changes as command signals. A link layer controller, that is located in the roadside, will calculate and communicate to the vehicles in the stretch of highway under its control speed and lane change commands in such a way that real traffic flow conditions approach the desired ones.

The determination of the desired traffic condition involves some form of optimization, and it is not a problem pursued in this paper. In Broucke and Varaiya (1996) a theory that can be used for the optimization is presented.

Three important differences with the results in Li et al. (1997a,b) and Alvarez et al. (1999) are presented here.

1. The structure of the control laws is now much simpler. In Li et al. (1997a,b) and Alvarez et al. (1999) a change of coordinates was used to calculate the stabilizing control law. This change of coordinates is not used and the stability is proved based only on gradients of weighted density errors. This reduces the complexity during implementation.
2. Inlet traffic flow conditions in Li et al. (1997a,b) and Alvarez et al. (1999) were assumed to match those of the desired traffic flow profiles. In this paper this condition is relaxed. When the desired and real traffic flow conditions are different in a highway section, the controller minimizes the overall density error in that section.
3. The desired rates of lane change can vary now with time as opposed to the results in Li et al. (1997a,b) where they were time independent.

The paper is divided in five sections. Section 2 contains the link layer controller design for a multi-lane single destination AHS, while Section 3 describes the controller for the multiple

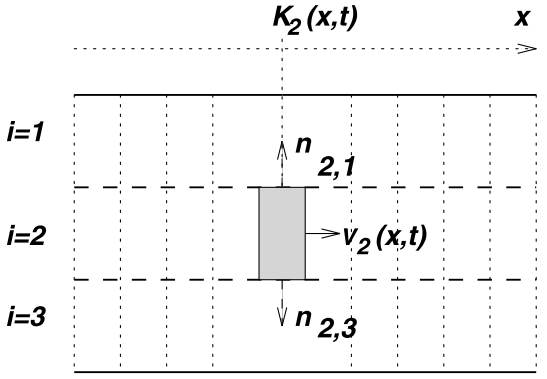

Fig. 2. Discrete lane highway model.

destination case. Simulation results are presented in Section 4, while Section 5 describes the conclusions of the work.

2. Discrete lanes highway

Consider a highway of length L, consisting of n lanes (in Fig. 2, $n = 3$). Using a principle of vehicles conservation, the dynamics of the vehicle density satisfy the following partial differential equation:

$$\frac{\partial \mathbf{K}(x,t)}{\partial t} = -\frac{\partial}{\partial x}\{\mathbf{V}(x,t)\mathbf{K}(x,t)\} + \mathbf{N}(x,t)\mathbf{K}(x,t), \tag{1}$$

where $\mathbf{K}(x,t) \in \mathscr{R}^n$, $K_i(x,t)$, the ith element, is the vehicle density on lane i, position $x \in [0,L] \subset \mathscr{R}$ and time t, $\mathbf{V}(x,t) \in \mathscr{R}^n \times \mathscr{R}^n$ is a diagonal matrix whose ith diagonal entry, $V_i(x,t)$, is the traffic flow velocity in lane i, and $\mathbf{N}(x,t) \in \mathscr{R}^n \times \mathscr{R}^n$ represents the proportion of vehicle density that is changing lanes per unit time at that particular position x and time t. The first term in the right hand side of Eq. (1) represents the inlet flow entering at location x and time t in the longitudinal direction of traffic, while the other term in this same side represents the inlet flow due to lane changes at this same location and time. [1] Traffic flow stabilization for the discrete lane highway is analyzed under the following assumption.

Assumption 1

1. The dynamics of the coordination and regulation layers are sufficiently fast and are capable of achieving velocity regulation.
2. The velocity $\mathbf{V}(x,t)$ and the proportion of lane change $\mathbf{N}(x,t)$ can be commanded.
3. Lane change is constrained to occur only between adjacent lanes, therefore the structure of $\mathbf{N}(x,t)$ is

[1] See Li et al. (1997a,b) for more details about this derivation.

$$\mathbf{N}(x,t)=\begin{bmatrix} -n_{1,2}(x,t) & n_{2,1}(x,t) & 0 & \cdots 0 \\ n_{1,2}(x,t) & -n_{2,1}(x,t)-n_{2,3}(x,t) & n_{3,2}(x,t) & \cdots 0 \\ 0 & n_{2,3}(x,t) & -n_{3,2}(x,t)-n_{3,4}(x,t) & \cdots 0 \\ & \vdots & & \\ 0, & \cdots & n_{n-1,n}(x,t) & -n_{n,n-1}(x,t) \end{bmatrix},$$

where $n_{i,j}(x,t)\geqslant 0;\ \forall i,j\in\{1,\ldots,n\}$ represents the proportion of vehicles changing from lane i to lane j per unit time, $n_{i,j}(x,t)=0\ \forall|i-j|>1$.

4. The desired velocity, proportion of change lane and density profiles, $\mathbf{V}_{\mathrm{d}}(x)$, $\mathbf{N}_{\mathrm{d}}(x,t)$ and $\mathbf{K}_{\mathrm{d}}(x,t)$, also satisfy a conservation of vehicles principle

$$\frac{\partial\mathbf{K}_{\mathrm{d}}(x,t)}{\partial t}=-\frac{\partial}{\partial x}\{\mathbf{V}_{\mathrm{d}}(x)\mathbf{K}_{\mathrm{d}}(x,t)\}+\mathbf{N}_{\mathrm{d}}(x,t)\mathbf{K}_{\mathrm{d}}(x,t), \tag{2}$$

with $\mathbf{K}_{\mathrm{d}}(x,t)$, $\mathbf{V}_{\mathrm{d}}(x)$ and $\mathbf{N}_{\mathrm{d}}(x,t)$ similarly defined to $\mathbf{K}(x,t)$, $\mathbf{V}(x,t)$ and $\mathbf{N}(x,t)$, respectively. The desired velocity is always positive, not dependent on time and can be different between lanes.

5. Only net changes of lane should be considered when specifying the matrix $\mathbf{N}_{\mathrm{d}}(x,t)$, that is

$$\text{if } n_{\mathrm{d}_{i,j}}(x,t)\neq 0\Rightarrow n_{\mathrm{d}_{j,i}}(x,t)=0;\quad |i-j|=1\quad \forall i,j\in\{1,\ldots,n\}.$$

Define the density error vector as

$$\widetilde{\mathbf{K}}(x,t)=\alpha\mathbf{K}_{\mathrm{d}}(x,t)-\mathbf{K}(x,t), \tag{3}$$

where $0<\alpha\leqslant\alpha_{\max}$. It should be noticed that Eq. (2) is still satisfied when $\mathbf{K}_{\mathrm{d}}(x,t)$ is substituted with $\alpha\mathbf{K}_{\mathrm{d}}(x,t)$. The choice of $\alpha_{\max}$ is such that Eq. (2) still satisfies highway capacity constraints for $\alpha_{\max}\mathbf{K}_{\mathrm{d}}(x,t)$. It is important to remark that this definition of the density error vector is different from the one introduced in Li et al. (1997a,b). The role of α is to allow the representation of differences between the desired and real traffic flow conditions. It is assumed that these differences will remain constant for a finite interval of time.

Decompose $\mathbf{V}(x,t)$ and $\mathbf{N}(x,t)$ as

$$\mathbf{V}(x,t)=\mathbf{V}_{\mathrm{d}}(x)+\mathbf{V}_{\mathrm{f}}(x,t), \tag{4}$$

$$\mathbf{N}(x,t)=\mathbf{N}_{\mathrm{d}}(x,t)+\mathbf{N}_{\mathrm{f}}(x,t). \tag{5}$$

By subtracting Eq. (1) from Eq. (2), the equation for the dynamics of the density error is

$$\frac{\partial\widetilde{\mathbf{K}}(x,t)}{\partial t}=-\frac{\partial}{\partial x}\left\{\mathbf{V}_{\mathrm{d}}(x)\widetilde{\mathbf{K}}(x,t)\right\}+\mathbf{N}_{\mathrm{d}}(x)\widetilde{\mathbf{K}}(x,t)+\frac{\partial}{\partial x}\{\mathbf{V}_{\mathrm{f}}(x,t)\mathbf{K}(x,t)\}-\mathbf{N}_{\mathrm{f}}(x,t)\mathbf{K}(x,t). \tag{6}$$

Define the feedback control law $\mathbf{V}_{\mathrm{f}}(x,t)$ by

$$\mathbf{V}_{\mathrm{f}}(x,t)=\gamma(x,t)\mathrm{diag}\left\{\frac{\partial}{\partial x}\{\mathbf{V}_{\mathrm{d}}(x)\widetilde{\mathbf{K}}(x,t)\}\right\}, \tag{7}$$

where $\gamma(x,t)\geqslant 0$ is a gain with $\gamma(0,t)=\gamma_i(L,t)=0$.

The (i,j)-element of the feedback control law matrix $\mathbf{N}_{\mathrm{f}}(x,t)$ is defined by

$$n_{\mathrm{f}_{i,j}}(x,t)=\begin{cases}-\zeta_{i,j}(x,t)(\widetilde{K}_i(x,t)V_{\mathrm{d}_i}(x)-\widetilde{K}_j(x,t)V_{\mathrm{d}_j}(x)); & |i-j|=1,\\ & \widetilde{K}_i(x,t)V_{\mathrm{d}_i}(x)<\widetilde{K}_j(x,t)V_{\mathrm{d}_j}(x),\\ 0; & \text{else},\end{cases} \tag{8}$$

where $\zeta_{i,j}(x,t)\geqslant 0$ is a gain.

Denote the $\mathscr{L}_2$ norm of the density error vector $\widetilde{\mathbf{K}}(\cdot,t)$ to be

$$\|\widetilde{\mathbf{K}}(\cdot,t)\|_2^2=\int_0^L \widetilde{\mathbf{K}}(x,t)^{\mathrm{T}}\widetilde{\mathbf{K}}(x,t)\,\mathrm{d}x.$$

The following theorem is presented.

Theorem 1. *Consider the discrete n-lane highway model in Eq.* (1) *and define the density error* $\widetilde{\mathbf{K}}(x,t)$ *as in Eq.* (3), *where* $0<\alpha\leqslant\alpha_{\max}$ *is given. Consider the control laws in Eqs.* (7) *and* (8) *under the conditions specified by Assumption* 1. *Then the equilibrium* $\widetilde{\mathbf{K}}(x,t)=0\ \forall x\in[0,L]$ *is stable in the* $\mathscr{L}_2$ *sense. Moreover, under the proposed control laws and for all* $0<\alpha\leqslant\alpha_{\max}$ *one of the following equilibria will be reached*

- *If the inlet flow condition satisfies* $\mathbf{V}(0,t)\mathbf{K}(0,t)=\alpha\mathbf{V}_{\mathrm{d}}(0)\mathbf{K}_{\mathrm{d}}(0,t)$

$$\widetilde{\mathbf{K}}(x,t)=\mathbf{0}. \tag{9}$$

- *If the inlet flow condition satisfies* $\mathbf{V}(0,t)\mathbf{K}(0,t)=\beta\mathbf{V}_{\mathrm{d}}(0)\mathbf{K}_{\mathrm{d}}(0,t);\ \beta\neq\alpha;\ 0<\beta\leqslant\alpha_{\max}$

$$\frac{\partial}{\partial x}\{\mathbf{V}_{\mathrm{d}}(x)\widetilde{\mathbf{K}}(x,t)\}=\mathbf{0}, \tag{10}$$

$$\widetilde{K}_i(x,t)V_{\mathrm{d}_i}(x)=\widetilde{K}_j(x,t)V_{\mathrm{d}_j}(x)\quad\forall i,j\in\{1,\ldots,n\}. \tag{11}$$

Proof. See Appendix A. □

Remark

1. The role of α in Theorem 1 is to allow differences between the real and desired inlet flows. When $\alpha=1$ the control laws proposed in Eqs. (7) and (8) allow perfect tracking of traffic flow along the highway. In most real traffic conditions, however, a value of $\alpha\neq 1$ is expected. In these situations it is impossible to achieve perfect density traffic along the highway. The controller then tries to track an scaled version of the density error that takes this difference into account. When $\alpha\neq 1$, $\widetilde{K}_i(x,t)=0$ does not imply $K_i(x,t)=K_{\mathrm{d}_i}(x,t)$.
2. Notice that the definition of the control laws in Eqs. (7) and (8) requires a priori knowledge of α. It is assumed that the real inlet flow conditions are measurable and therefore that the value of α can be deduced by comparing real and desired inlet flow conditions. It is also assumed that α is bounded and remains constant for a finite interval of time. In practice, this requirement implies that the changes in the value of α are slower than the dynamics of the traffic flow controller.
3. Theorem 1 also guarantees that when the α used in control laws in Eqs. (7) and (8) does not coincide with the true factor β that matches the difference between the real and desired inlet flows, i.e., when $\mathbf{V}(0,t)\mathbf{K}(0,t)=\beta\mathbf{V}_{\mathrm{d}}(0)\mathbf{K}_{\mathrm{d}}(0,t);\ \beta\neq\alpha;0<\beta\leqslant\alpha_{\max}$ then the equilibria that will

be reached is such that the gradients of the weighted density errors will be zero in both the longitudinal direction and across lanes.

4. When the equilibria in Theorem 1 are reached, the following conditions are satisfied

$$\lim_{t\to\infty} \mathbf{V}(x,t) = \mathbf{V}_{\mathrm{d}}(x),$$
$$\lim_{t\to\infty} \mathbf{V}_{\mathrm{f}}(x,t) = 0,$$
$$\lim_{t\to\infty} \mathbf{N}_{\mathrm{f}}(x,t) = 0,$$

this implies that the controller forces the desired and real velocities to coincide and therefore the feedback terms $\mathbf{V}_{\mathrm{f}}(x,t)$ and $\mathbf{N}_{\mathrm{f}}(x,t)$ eventually vanish.

3. Multi-destination traffic discrete lanes highway

Consider a n-lane highway in which vehicles with different destinations are sharing lanes. Vehicles with the same final destination can be associated with a particular index or color. Using a principle of vehicles conservation, the dynamics of the vehicle density for each color satisfy the following partial differential equation:

$$\frac{\partial \mathbf{K}^c(x,t)}{\partial t} = -\frac{\partial}{\partial x}\{\mathbf{V}^c(x,t)\mathbf{K}^c(x,t)\} + \mathbf{N}^c(x,t)\mathbf{K}^c(x,t), \tag{12}$$

where $\mathbf{K}^c(x,t) \in \mathscr{R}^n$, $K_i^c(x,t)$, the ith element, is the vehicle density of color c on lane i, position $x \in x \in [0,L] \subset \mathscr{R}$ and time t, $\mathbf{V}^c(x,t) \in \mathscr{R}^n \times \mathscr{R}^n$ is a diagonal matrix whose ith diagonal entry is the traffic flow velocity of color c in lane i, and $\mathbf{N}^c(x,t) \in \mathscr{R}^n \times \mathscr{R}^n$ represents the proportion of vehicle density of color c that is changing lanes per unit time at that particular position x and time t. Traffic flow stabilization for the multi-destination discrete lane highway is analyzed under the following assumption.

Assumption 2

1. The velocity $\mathbf{V}^c(x,t)$ and the proportion of lane change $\mathbf{N}^c(x,t)$ can be commanded.
2. Lane change is constrained to occur only between adjacent lanes, therefore the structure of $\mathbf{N}^c(x,t)$ is

$$\mathbf{N}^c(x,t) = \begin{pmatrix} -n_{1,2}^c(x,t) & n_{2,1}^c(x,t) & 0 & \dots 0 \\ n_{1,2}^c(x,t) & -n_{2,1}^c(x,t) - n_{2,3}^c(x,t) & n_{3,2}^c(x,t) & \dots 0 \\ 0 & n_{2,3}^c(x,t) & -n_{3,2}^c(x,t) - n_{3,4}^c(x,t) & \dots 0 \\ & \vdots & & \\ 0 & \dots & n_{n-1,n}^c(x,t) & -n_{n,n-1}^c(x,t) \end{pmatrix},$$

where $0 \leqslant n_{i,j}^c(x,t) \leqslant 1 \ \forall i,j \in \{1,\dots,n\}$ represents the proportion of vehicles changing from lane i to lane j per unit time. Notice that $n_{i,j}^c(x,t) = 0 \ \forall |i-j| > 1$.

3. The desired velocity, proportion of change lane and density profiles, $\mathbf{V}_{\mathrm{d}}^c(x)$, $\mathbf{N}_{\mathrm{d}}^c(x)$ and $\mathbf{K}_{\mathrm{d}}^c(x,t)$, satisfy

$$\frac{\partial \mathbf{K}_{\mathrm{d}}^{c}(x,t)}{\partial t} = -\frac{\partial}{\partial x}\{\mathbf{V}_{\mathrm{d}}^{c}(x)\mathbf{K}_{\mathrm{d}}^{c}(x,t)\} + \mathbf{N}_{\mathrm{d}}^{c}(x,t)\mathbf{K}_{\mathrm{d}}^{c}(x,t), \tag{13}$$

with $\mathbf{K}_{\mathrm{d}}^{c}(x,t)$, $\mathbf{V}_{\mathrm{d}}^{c}(x)$ and $\mathbf{N}_{\mathrm{d}}^{c}(x,t)$ similarly defined to $\mathbf{K}^{c}(x,t)$, $\mathbf{V}^{c}(x,t)$ and $\mathbf{N}^{c}(x,t)$, respectively. The desired traffic flow profile must be physically realizable.

4. Only net changes of lane are considered when specifying the matrix $\mathbf{N}_{\mathrm{d}}^{c}(x,t)$, that is

$$\text{if } n_{\mathrm{d}_{i,j}}^{c}(x,t) \neq 0 \Rightarrow n_{\mathrm{d}_{j,i}}^{c}(x,t) = 0; \quad |i-j| = 1 \ \ \forall i,j \in \{1,\ldots,n\}.$$

5. Vehicles do not change destination or color, once assigned.

Define the vectors and matrices

$$\begin{aligned}
\mathbf{K}_{\omega}(x,t) &= \left[\mathbf{K}^{1}(x,t)^{\mathrm{T}},\ldots,\mathbf{K}^{m}(x,t)^{\mathrm{T}}\right]^{\mathrm{T}},\\
\mathbf{V}_{\omega}(x,t) &= \mathrm{diag}\left\{\mathbf{V}^{1}(x,t),\ldots,\mathbf{V}^{m}(x,t)\right\},\\
\mathbf{N}_{\omega}(x,t) &= \mathrm{diag}\left\{\mathbf{N}^{1}(x,t),\ldots,\mathbf{N}^{m}(x,t)\right\},\\
\mathbf{K}_{\omega_{\mathrm{d}}}(x,t) &= \left[\mathbf{K}_{\mathrm{d}}^{1}(x,t)^{\mathrm{T}},\ldots,\mathbf{K}_{\mathrm{d}}^{m}(x,t)^{\mathrm{T}}\right]^{\mathrm{T}},\\
\mathbf{V}_{\omega_{\mathrm{d}}}(x) &= \mathrm{diag}\left\{\mathbf{V}_{\mathrm{d}}^{1}(x),\ldots,\mathbf{V}_{\mathrm{d}}^{m}(x)\right\},\\
\mathbf{N}_{\omega_{\mathrm{d}}}(x,t) &= \mathrm{diag}\left\{\mathbf{N}_{\mathrm{d}}^{1}(x,t),\ldots,\mathbf{N}_{\mathrm{d}}^{m}(x,t)\right\},
\end{aligned}$$

where m is the total number of different destinations. The vehicle density dynamics for all colors can be expressed as

$$\frac{\partial \mathbf{K}_{\omega}(x,t)}{\partial t} = -\frac{\partial}{\partial x}\{\mathbf{V}_{\omega}(x,t)\mathbf{K}_{\omega}(x,t)\} + \mathbf{N}_{\omega}(x,t)\mathbf{K}_{\omega}(x,t) \tag{14}$$

and the desired velocity, proportion of change lane and density profiles for all color as

$$\frac{\partial \mathbf{K}_{\omega_{\mathrm{d}}}(x,t)}{\partial t} = -\frac{\partial}{\partial x}\left\{\mathbf{V}_{\omega_{\mathrm{d}}}(x)\mathbf{K}_{\omega_{\mathrm{d}}}(x,t)\right\} + \mathbf{N}_{\omega_{\mathrm{d}}}(x,t)\mathbf{K}_{\omega_{\mathrm{d}}}(x,t). \tag{15}$$

Define the density error vector as

$$\widetilde{\mathbf{K}}_{\omega}(x,t) = \alpha_{\omega_{\mathrm{d}}}\mathbf{K}_{\omega_{\mathrm{d}}}(x,t) - \mathbf{K}_{\omega}(x,t), \tag{16}$$

where $\alpha_{\omega_{\mathrm{d}}}$ is a diagonal matrix with each one of its entries defined similarly to α in the single destination case. Decompose $\mathbf{V}_{\omega}(x,t)$ and $\mathbf{N}_{\omega}(x,t)$ as

$$\mathbf{V}_{\omega}(x,t) = \mathbf{V}_{\omega_{\mathrm{d}}}(x) + \mathbf{V}_{\omega_{\mathrm{f}}}(x,t), \tag{17}$$

$$\mathbf{N}_{\omega}(x,t) = \mathbf{N}_{\omega_{\mathrm{d}}}(x,t) + \mathbf{N}_{\omega_{\mathrm{f}}}(x,t). \tag{18}$$

By subtracting Eqs. (15) and (14) and using (17) and (18) the equation for the dynamics of the density error is

$$\begin{aligned}
\frac{\partial \widetilde{\mathbf{K}}_{\omega}(x,t)}{\partial t} = &-\frac{\partial}{\partial x}\left\{\mathbf{V}_{\omega_{\mathrm{d}}}(x)\widetilde{\mathbf{K}}_{\omega}(x,t)\right\} + \mathbf{N}_{\omega_{\mathrm{d}}}(x)\widetilde{\mathbf{K}}_{\omega}(x,t) + \frac{\partial}{\partial x}\left\{\mathbf{V}_{\omega_{\mathrm{f}}}(x,t)\mathbf{K}_{\omega}(x,t)\right\}\\
&- \mathbf{N}_{\omega_{\mathrm{f}}}(x,t)\mathbf{K}_{\omega}(x,t).
\end{aligned} \tag{19}$$

To deal with the special conditions imposed by multi-destination traffic control, the following additional assumption is introduced.

Assumption 3

1. The velocity that is commanded to vehicles that are sharing the same lane is independent of their destination, i.e.,

$$\mathbf{V}(x,t) = \mathbf{V}^1(x,t) = \mathbf{V}^2(x,t) = \cdots = \mathbf{V}^m(x,t).$$

2. It is allowed to command different proportions of lane changes to vehicles with different destinations that are sharing the same lane, i.e., in general

$$\mathbf{N}^1(x,t) \neq \mathbf{N}^2(x,t) \neq \cdots \neq \mathbf{N}^m(x,t).$$

Notice that assumption in 3.1 is important not only for practical reasons, but also from a safety point of view. It is necessary to avoid that vehicles with different destination are trying to overrun each other in the same lane.

To define the feedback control laws $\mathbf{V}_{\mathrm{f}}(x,t)$ and $\mathbf{N}_{\mathrm{f}}(x,t)$ first define the vectors

$$\mathbf{F}_{\omega}(x,t) = [\mathbf{F}^1(x,t),\ldots,\mathbf{F}^m(x,t)] = \frac{\partial}{\partial x}\left\{\widetilde{\mathbf{K}}_{\omega}(x,t)^{\mathrm{T}}\mathbf{V}_{\omega_{\mathrm{d}}}(x)\right\} \tag{20}$$

and

$$\mathbf{H}_{\omega}(x,t) = [\mathbf{H}^1(x,t),\ldots,\mathbf{H}^m(x,t)] = \widetilde{\mathbf{K}}_{\omega}(x,t)^{\mathrm{T}}\mathbf{V}_{\omega_{\mathrm{d}}}(x). \tag{21}$$

The ith element of the diagonal matrix $\mathbf{V}_{\omega_{\mathrm{f}}}(x,t)$ is given by

$$V_{\omega_{\mathrm{f}_i}}(x,t) = \gamma_i(x,t)\left[F_i^1(x,t)K_i^1(x,t) + \cdots + F_i^m(x,t)K_i^m(x,t)\right], \tag{22}$$

where $\gamma_i(x,t) \geqslant 0$ is a gain with $\gamma_i(0,t) = \gamma_i(L,t) = 0$ and $F_i^c(x,t)$ is the ith element of $\mathbf{F}^c(x,t)$ in Eq. (20).

In the case of the matrix $\mathbf{N}_{\omega_{\mathrm{f}}}(x,t)$, from (18) it follows that its structure is

$$\mathbf{N}_{\omega_{\mathrm{f}}}(x,t) = \mathrm{diag}\left\{\mathbf{N}_{\mathrm{f}}^1(x,t),\ldots,\mathbf{N}_{\mathrm{f}}^m(x,t)\right\}.$$

According with Assumption 3, the matrices $\mathbf{N}_{\mathrm{f}}^c(x,t)$ must have the same structure of $\mathbf{N}_{\mathrm{d}}^c(x,t)\ \forall c \in \mathbf{N}_{\mathrm{d}}^c(x,t)\ \forall c \in \{1,\ldots,m\}$ to allow changes of lane only between adjacent lanes. Their (i,j)-element is defined as

$$n_{\mathrm{f}_{i,j}}^c(x,t) = \begin{cases} -\zeta_{i,j}^c(x,t)(h_i^c(x,t) - h_j^c(x,t)); & |i-j| = 1, \\ & h_i^c(x,t) > h_j^c(x,t), \\ 0; & \text{else}, \end{cases} \tag{23}$$

where $\zeta_{i,j}^c(x,t) \geqslant 0$ is a gain and $h_j^c(x,t)$ is the jth element of $\mathbf{H}^c(x,t)$ in Eq. (21).

Denote the $\mathscr{L}_2$ norm of the density error vector $\widetilde{\mathbf{K}}_{\omega}(\cdot,t)$ to be

$$\|\widetilde{\mathbf{K}}_{\omega}(\cdot,t)\|_2^2 = \int_0^L \widetilde{\mathbf{K}}_{\omega}(x,t)^{\mathrm{T}}\widetilde{\mathbf{K}}_{\omega}(x,t)\,\mathrm{d}x.$$

The main result of this paper is now presented.

Theorem 2. *Consider the discrete n-lane highway model in Eq.* (14) *and define the density error* $\widetilde{\mathbf{K}}_\omega(x,t)$ *as in Eq.* (16), *where* $0 < \alpha \leqslant \alpha_{\max}$ *is given. Consider the control laws in Eqs.* (22) *and* (23) *under the conditions specified by Assumptions* 1–3. *Then the equilibrium* $\widetilde{\mathbf{K}}_\omega(x,t) = \mathbf{0}\ \forall x \in [0,L]$ *is* $\mathscr{L}_2$ *stable.*

Moreover, under the proposed control laws and for all $0 < \alpha \leqslant \alpha_{\max}$ *one of the following equilibria will be reached*

- *If the inlet flow condition satisfies* $\mathbf{V}_\omega(0,t)\mathbf{K}_\omega(0,t) = \alpha_{\omega_\mathrm{d}}\mathbf{V}_{\omega_\mathrm{d}}(0)\mathbf{K}_{\omega_\mathrm{d}}(0,t)$

$$\widetilde{\mathbf{K}}_\omega(x,t) = \mathbf{0}. \tag{24}$$

- *If the inlet flow condition satisfies* $\mathbf{V}_\omega(0,t)\mathbf{K}_\omega(0,t) = \beta_{\omega_\mathrm{d}}\mathbf{V}_{\omega_\mathrm{d}}(0)\mathbf{K}_{\omega_\mathrm{d}}(0,t)$ *where* $\beta_{\omega_\mathrm{d}} = \mathrm{diag}\{\beta,\ldots,\beta\}$ *and* $\beta \neq \alpha$, $0 < \beta \leqslant \alpha_{\max}$.

$$\frac{\partial}{\partial x}\left\{\mathbf{V}_{\omega_\mathrm{d}}(\tilde{x})\mathbf{K}_\omega(x,t)\right\} = \mathbf{0}, \tag{25}$$

$$\widetilde{K}_i^c(x,t)^c V_{\mathrm{d}_i}^c(x) = \widetilde{K}_j^c(x,t)V_{\mathrm{d}_j}^c(x) \quad \forall i,j \in \{1,\ldots,n\},\ \ c \in \{1,\ldots,m\}. \tag{26}$$

Proof. See Appendix B. □

Remark. All remarks to Theorem 1 also apply to Theorem 2.

4. Link layer simulation results

To illustrate the effectiveness of the link layer controller, some simulation results are shown. The first set of results corresponds to the implementation on SmartPath (Eskafi et al., 1992) of the control laws in Eqs. (22) and (23), for the case of one destination. The second set corresponds to Matlab simulations results for the case of vehicles with multiple destinations. Finally the third set was obtained with SmartCap (Broucke et al., 1996) a meso-scale traffic simulator. It is important to remark that although the gains for the control laws, namely γ, $\zeta_{i,j}(x,t)$ $\gamma_i(x,t)$ and $\zeta_{i,j}^c(x,t)$ in Eqs. (7), (8), (22) and (23), respectively, can be time dependent, in the simulation results presented in this section a constant value was used for all positions x and times t. The simulation results were obtained after manually tunning the gains and represent typical simulation results.

4.1. SmartPath simulation results

SmartPath (Eskafi et al., 1992) is a comprehensive simulator for the hierarchical PATH AHS architecture. Simulations are executed based on a user provided file that contains information about the highway topology. Highways are partitioned into sections with specified geometry: length, curvature, banking, number of lanes, width of lanes, etc. A set of pointers defines the order in which the different sections and lanes are connected.

SmartPath includes routines to populate the highway with vehicles. These routines can create an initial set of vehicles to perform the simulation, or create vehicles during the course of the simulation. Maximum platoon size must be provided.

Independent coordination and regulation layers are created for each vehicle. The maximum number of vehicles in a single simulation is only limited by the time the corresponding simulation takes to complete. One important motivation to testing the link layer controller in SmartPath is that it is possible to validate the assumptions on the dynamics of coordination and regulation layers that were made while deriving the link layer model, namely fast dynamics as compared to the link layer.

SmartPath includes a communications module that handles all information interchange among vehicles and between vehicles and the highway infrastructure. All the layers are assumed to use this module to place or retrieve information.

SmartPath simulates the roadside infrastructure in such a way that the number of vehicles in lane and sections is known. Vehicular density is determined based on this information together with the length of the section. The longitudinal speed and the actual number of changes of lane that is to be executed in a given lane and section is supposed to be broadcasted by the highway infrastructure to the platoon leaders.

To establish the desired vehicular density and velocity profiles, special routines were developed for these simulations. These routines will to be substituted in a near future by a generator of desired traffic profiles, based on (Broucke and Varaiya, 1996).

SmartPath simulations were performed for one and two lane highways. In both cases an oval shaped track was used. The length of the oval is approximately of 5 km. There are about 100 vehicles per lane traveling at a nominal speed of 25 m/s. The circulation is in the counterclockwise direction.

The objective in the one lane simulation is to test the ability of the link layer controller to empty sections of highway. This capability is important in AHS systems because, for example, it provides space for vehicles entry to the AHS. The desired density distribution is illustrated in Fig. 3.

Figs. 4–6 show the simulation results for a one lane highway. Each block on Figs. 4–6 represents a platoon of vehicles including the headway of its leader, 60 m in these simulations. As Fig. 4 clearly illustrates, after 160 s there are large empty sections of highway in the two straight sections of the oval highway. It should be noticed that there is a reduction in the number of platoons, and therefore in the occupancy of the highway, due to the regulation and coordination layer control laws that enforce the occurrence of joins. The size of the empty sections is much larger that the one that can be obtained without the use of the link layer controller proposed here.

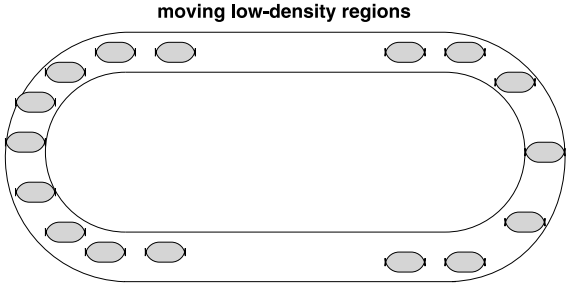

Fig. 3. SmartPath one lane simulation. Desired low density region.

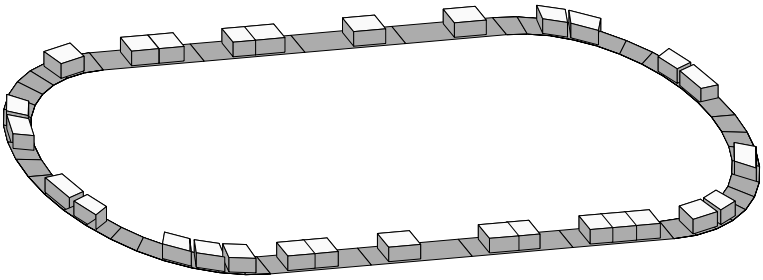

Fig. 4. SmartPath one lane simulation results $t = 0$ s.

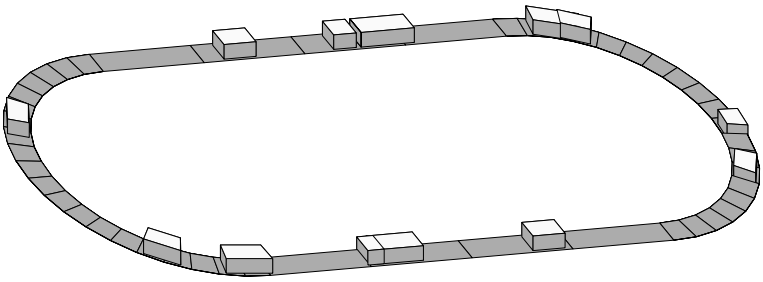

Fig. 5. SmartPath one lane simulation results $t = 80$ s.

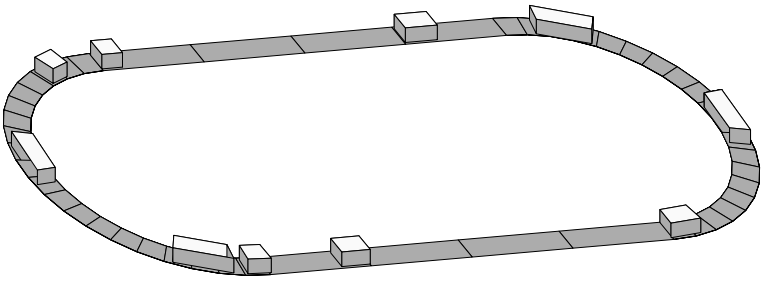

Fig. 6. SmartPath one lane simulation results $t = 160$ s.

In the case of the two lane SmartPath simulation, the link layer controller was required to perform two different tasks. The first task, which takes place in the lower straight section of the oval highway, consists of homogenizing the vehicle density on both lanes. The second task is to empty the inner lane of the highway at the end of the upper straight section of the oval. The desired situation is illustrated in Figs. 7 and 8. The simulation results are presented in Figs. 8–11.

The results in Figs. 9–11, that correspond to 40, 80 and 120 s of simulation time respectively, indicate that the link layer controller performed the two tasks successfully.

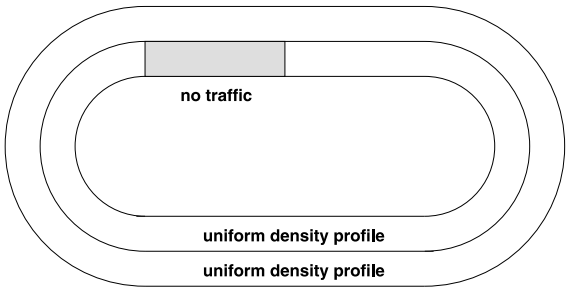

Fig. 7. SmartPath two lane simulation. Desired density regions.

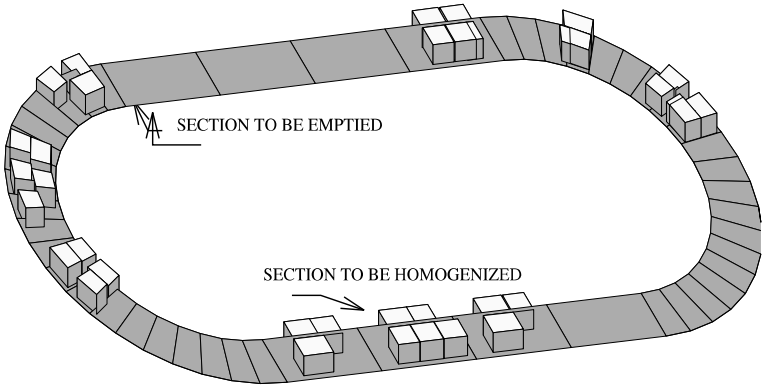

Fig. 8. SmartPath two lane simulation results $t = 0$ s.

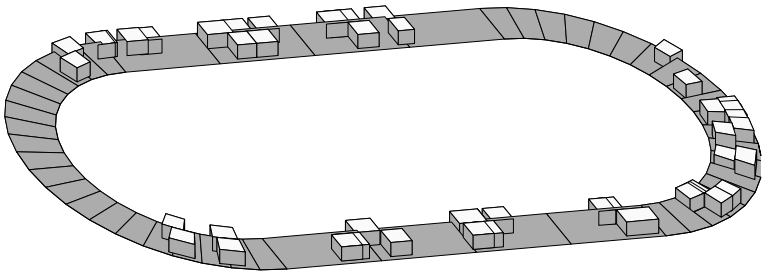

Fig. 9. SmartPath two lane simulation results $t = 40$ s.

4.2. Matlab simulation results

The second set of results corresponds to Matlab simulations of the control laws in Eqs. (22) and (23) for the case when vehicles which have two different destinations are traveling on a two lane highway. Figs. 12 and 13 show the desired density profiles for the two colors. At the beginning of the highway the desired behavior corresponds to vehicles of both colors mixed homogeneously in both lanes. At the middle of the stretch of highway, each lane should only contain vehicles of one color. At the end of the stretch of highway, the desired conditions are the same as those in the beginning.

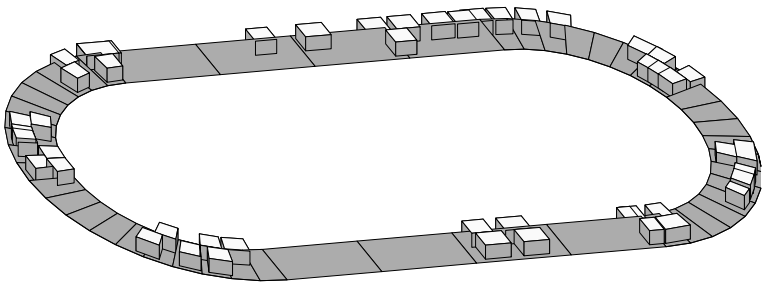

Fig. 10. SmartPath two lane simulation results $t = 80$ s.

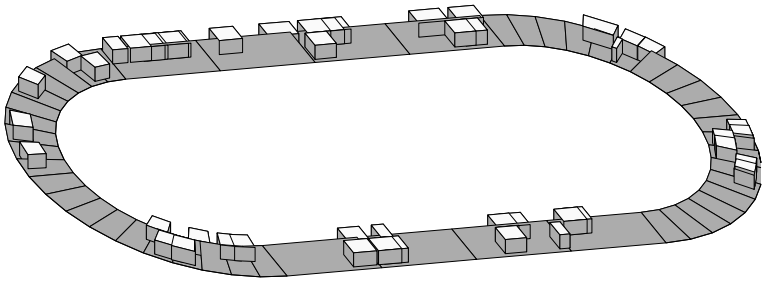

Fig. 11. SmartPath two lane simulation results $t = 120$ s.

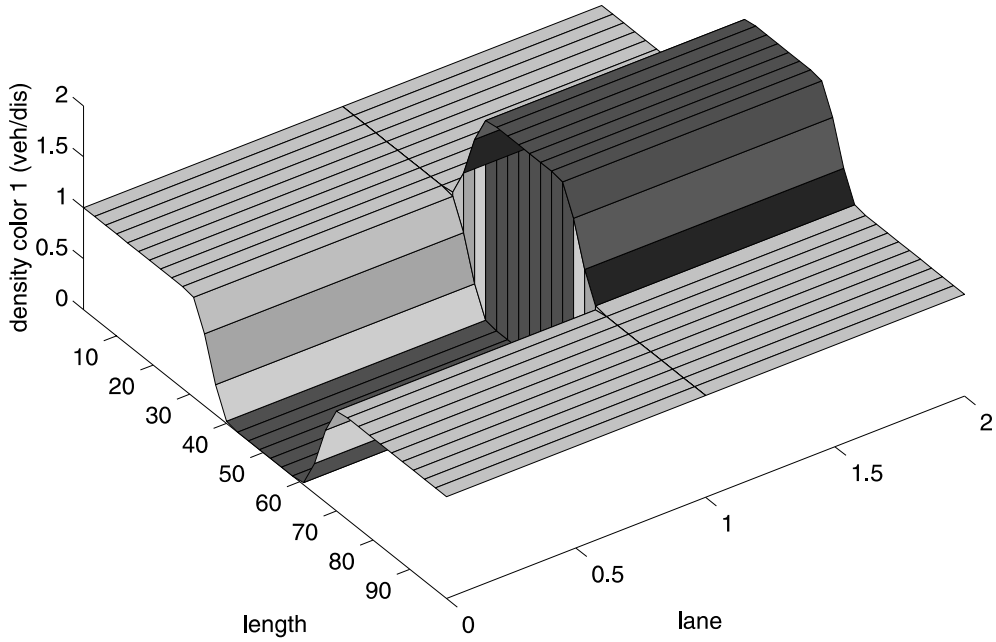

Fig. 12. Matlab two lane simulation results. Color 1 desired density.

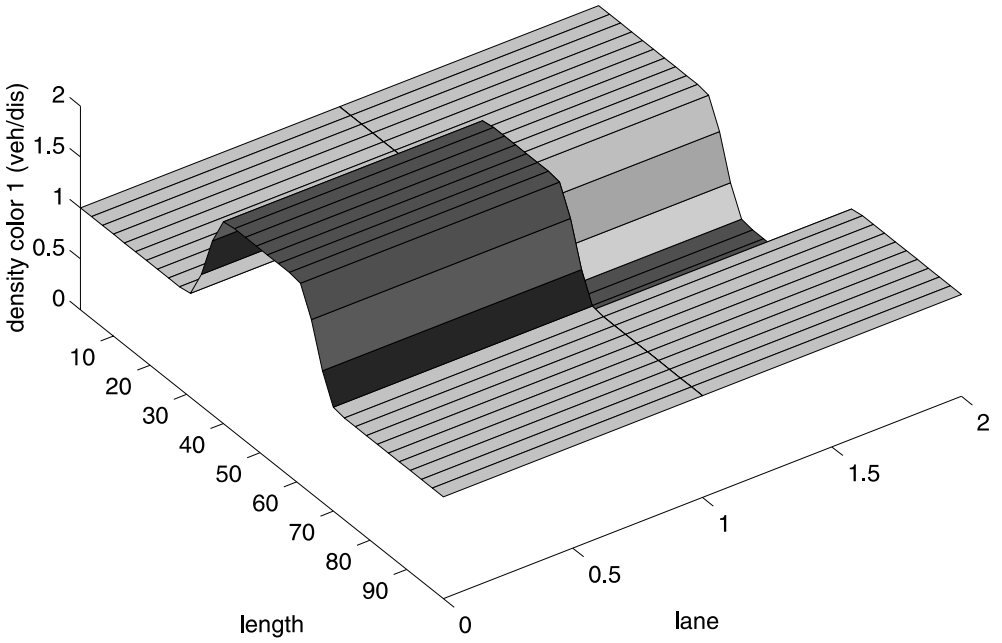

Fig. 13. Matlab two lane simulation results. Color 2 desired density.

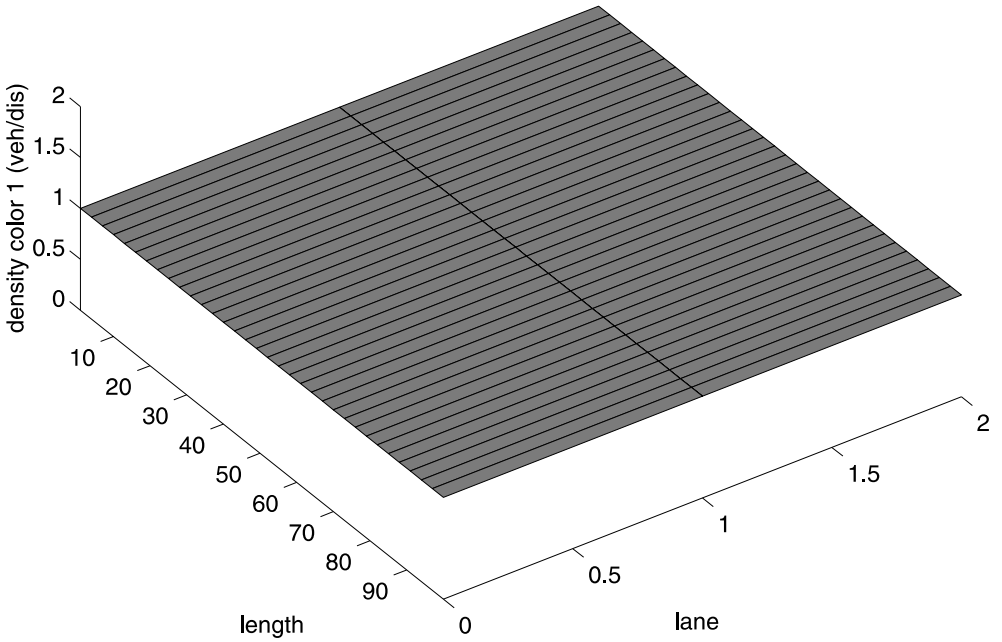

Fig. 14. Matlab two lane simulation results. Colors 1 and 2, $t = 0$.

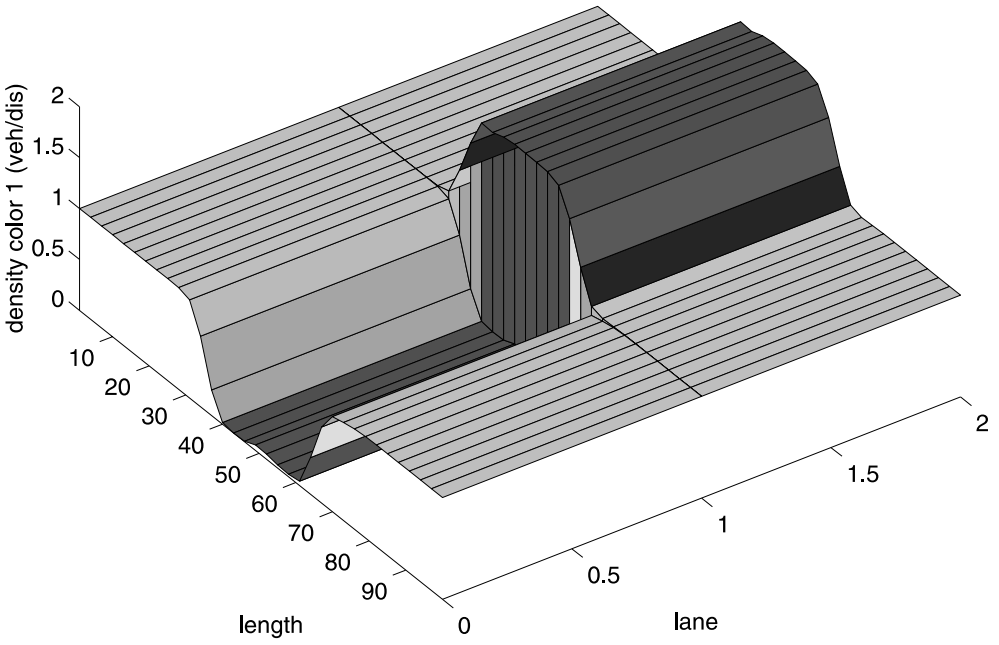

Fig. 15. Matlab two lane simulation results. Color 1, $t = 9$.

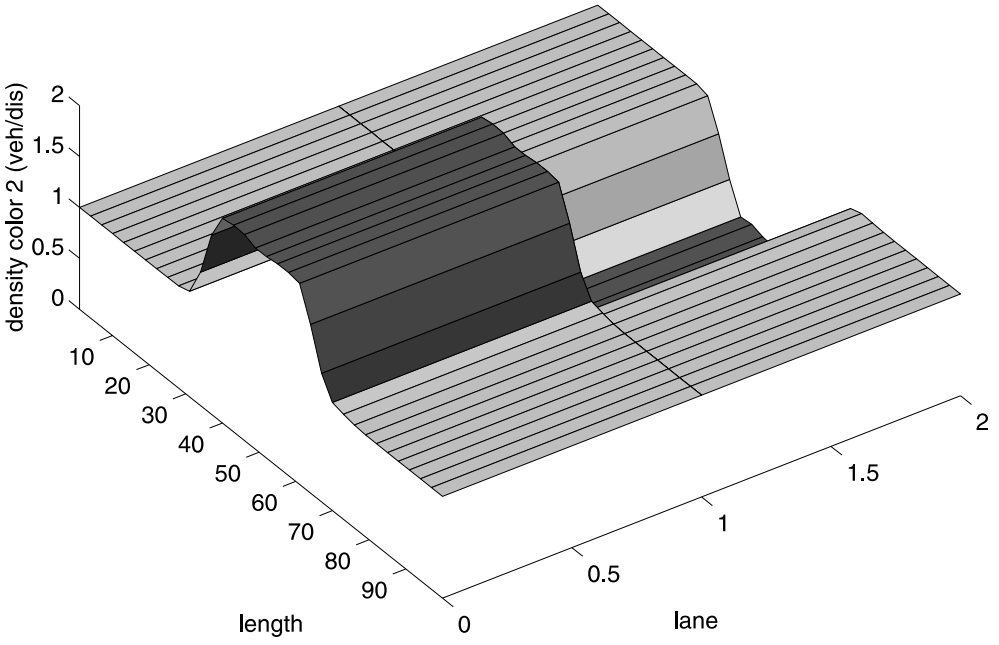

Fig. 16. Matlab two lane simulation results. Color 2, $t = 9$.

Fig. 14 shows the initial state for the simulation, which corresponds to an homogeneous mixture of the two colors along all the stretch of highway. Figs. 15 and 16 illustrate the simulation

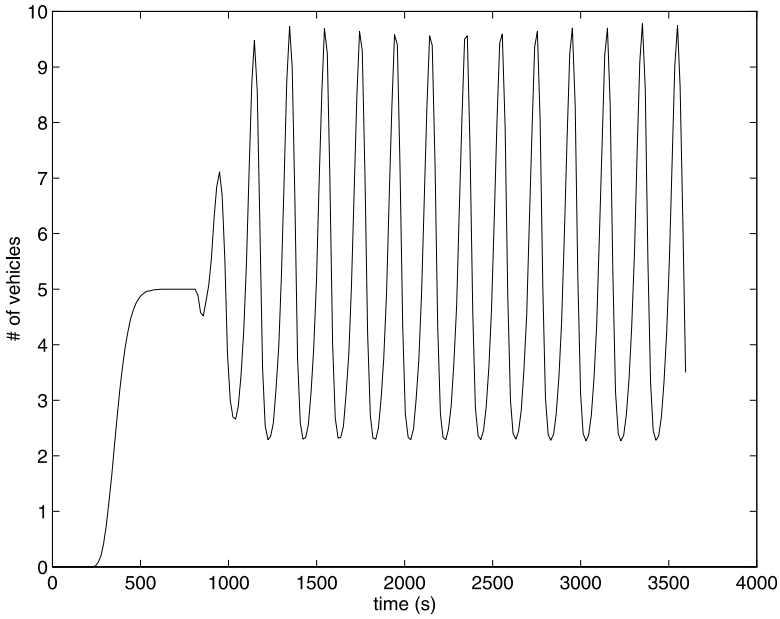

Fig. 17. SmartCap one lane highway simulation results: number of vehicles in the 15th section.

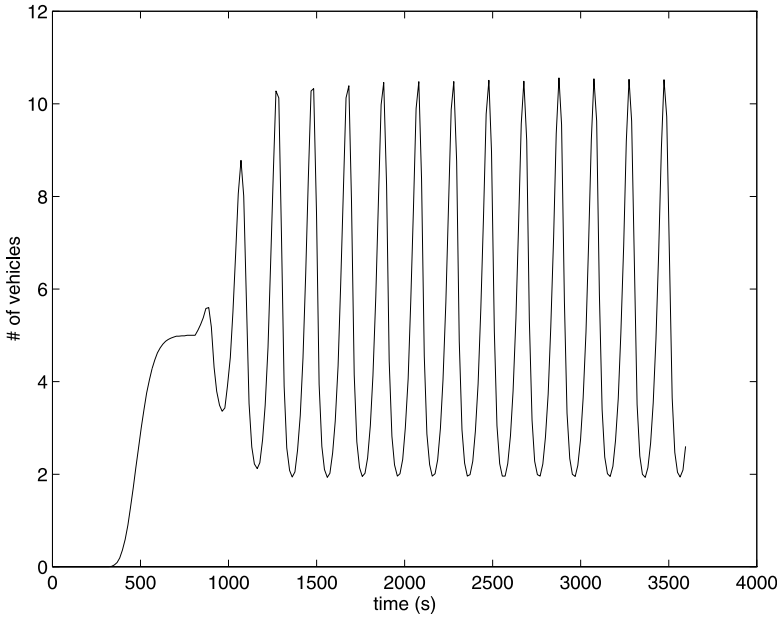

Fig. 18. SmartCap one lane highway simulation results: number of vehicles in the last section.

results after $t = 9$ units of simulation time. It is clear from these figures that the multi-destination link layer controller achieved a color density profile very close to the desired one.

It should be noticed that in a real highway there are many different destinations. However, it is possible to tag vehicles traveling to distant exits with just one color. Following the suggestion in Rao and Varaiya (1994) to allow vehicles only one lane change per highway section, the required number of different colors is related to the number of lanes in the AHS. In this case the computational complexity required to implement the multi-destination link layer controller remains small.

4.3. SmartCap simulation results

Two examples of simulation results obtained with SmartCap (Broucke et al., 1996) are included. SmartCap is a meso-scale traffic simulation package whose main advantage is the use of the notion of activities (Broucke and Varaiya, 1996). By using this notion it is possible to encode the space–time demands of vehicles while traveling in the highway and to consider bounds on the highway capacity. A proper selection of the space–time demands makes it possible to abstract the dynamics of the coordination and regulation layers and to reduce the simulation time demanded by a micro-scale simulator.

The first simulation example is a one lane highway in which vehicles are entering at the beginning of the highway at a constant rate. The control law in Eqs. (7) and (8) is applied to conform the uniform entry flow of vehicles into groups of vehicles, in such a way that empty highway space is created between these groups. This effect of producing empty sections on the highway can not be achieved with other types of traffic flow controllers, for example, like the

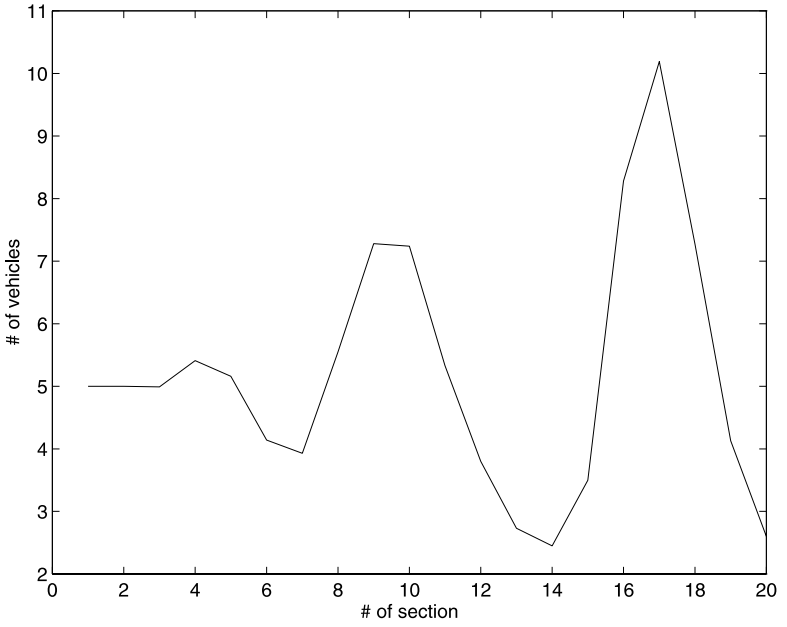

Fig. 19. SmartCap one lane highway simulation results: number of vehicles along the highway at the end of simulation time.

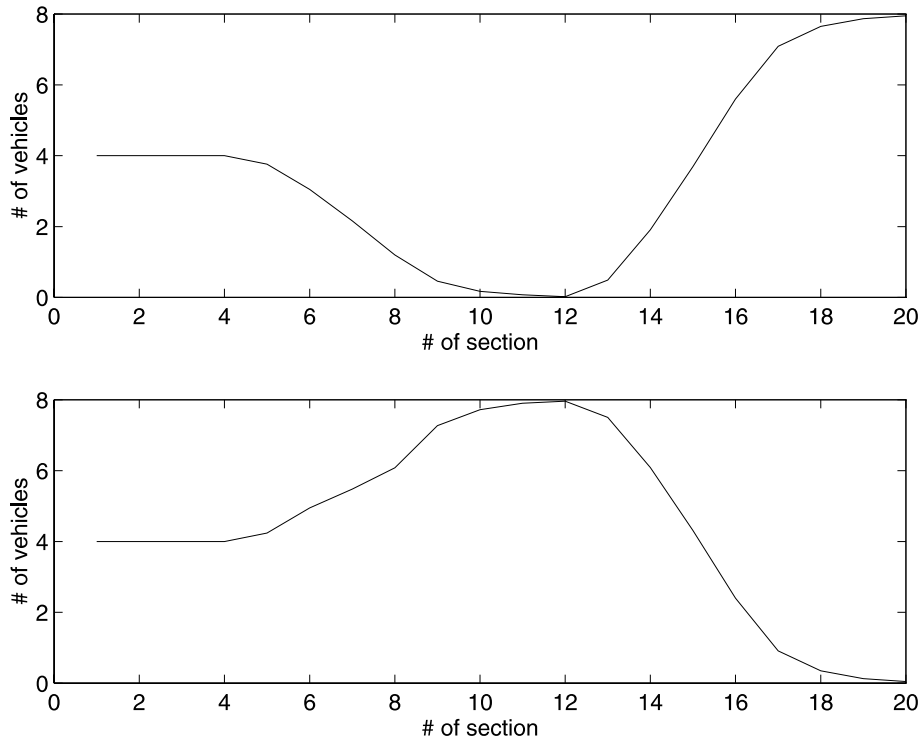

Fig. 20. SmartCap two lane simulation results: number of vehicles in the left lane at the end of the simulation. Top plot: vehicles with left lane destination. Bottom plot: vehicles with right lane destination.

greedy rule in Broucke and Varaiya (1996). The desired density for the groups of vehicles that are formed with the use of the controller in Eqs. (7) and (8) satisfies highway capacity constraints.

The second simulation example is a two lane highway. Vehicles enter the highway at a constant rate at the beginning of the highway using the two lanes. Half of the vehicles that enter the highway in each lane are bound to finish their trip in the left lane at the end of the highway and the other half needs to finish their trip in the right lane. Vehicles are required to switch to their final destination lane two times before they reach the end of the highway. Although in the normal scenario of destination control, only one change of lane is expected, this scenario of double lane change was chosen to emphasize the capabilities of the controller. The initial distribution of traffic on the highway is such that without the intervention of the control laws the desired traffic condition can not be achieved.

The highways are 10 km long in both cases partitioned in 500 m sections. Vehicles are assigned a desired constant speed of 20 m/s. Each section has a maximum capacity of 10.5 vehicles, according with the spacing policy adopted for the simulation.

Figs. 17 and 18 show the number of vehicles in the fifteenth and last section of the one lane highway as time passes. It can be noticed that the density varies significantly in the sections, indicating the success of the control law. Fig. 19 shows the distribution of vehicles at the end of

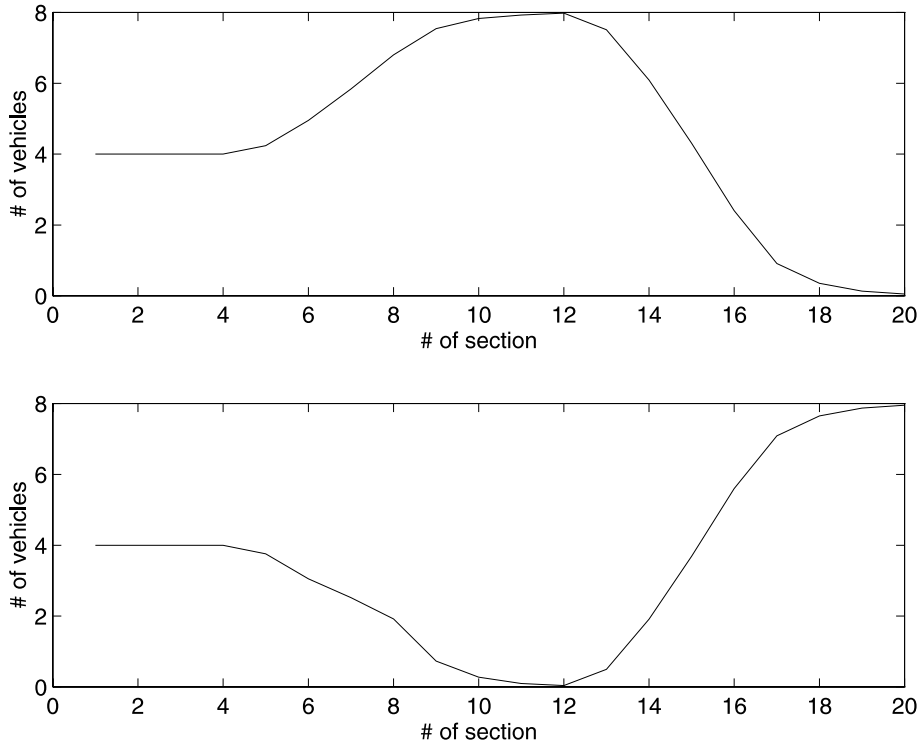

Fig. 21. SmartCap two lane simulation results: number of vehicles in the right lane at the end of the simulation. Top plot: vehicles with left lane destination. Bottom plot: vehicles with right lane destination.

the simulation. Notice that the inlet flow in the highway was kept constant and equal to the desired inlet flow. It can be noted that the controller is not producing overflow in any section.

Figs. 20 and 21 show the simulation results for the left lane and right lane, respectively, for the two lanes example. The convergence to the desired traffic conditions was accomplished in 50 s (that corresponded with three sampling times) for the entire highway.

5. Conclusions

This paper presents results on the traffic control of the hierarchical architecture of the PATH AHS presented in Varaiya and Shladover (1991). The main contributions are to traffic flow stabilization in the link layer level of this architecture.

The traffic of vehicles with different destination although sharing a multiple lane highway is considered. Assuming that the velocity and the lane change of vehicles in a stretch of highway can be commanded, a set of control laws that stabilize the vehicular traffic flow to predetermined desired profiles of velocity and density is presented.

The controller is derived from a model based on the principle of vehicles conservation and is based on Lyapunov stability results. The more important features of this controller are

- It is suitable for distributed implementation because it requires only local traffic information.
- It avoids traffic flow dynamics inversion that produce unbounded controls signals for small vehicular densities.
- It tracks the vehicle density profile that minimizes the error along all the stretch of highway, even when there is a mismatch between the desired and real inlet traffic flow.

The desired velocity and density profiles that are considered included the cases in which different desired velocities can be assigned to sections of the highway where lane change is supposed to occur. These profiles can be designed using the methodologies suggested in Broucke and Varaiya (1996) and Alvarez et al. (1998).

Simulation results are presented in Matlab, SmartPath (Eskafi et al., 1992) and SmartCap (Broucke et al., 1996). The simulation results indicate both, the validity of the assumptions about the dynamics of the coordination and regulation layers, and the effectiveness of the link layer controller.

Acknowledgements

Research supported by UCB-ITS PATH grants MOU-238, MOU-287, MOU-310 and MOU-311.

Appendix A. Proof of Theorem 1

Proof. Choose the following Lyapunov function candidate

$$U(t) = \frac{1}{2}\int_0^L \widetilde{\mathbf{K}}(x,t)^{\mathrm{T}}\mathbf{V}_{\mathrm{d}}(x)\widetilde{\mathbf{K}}(x,t)\,\mathrm{d}x. \tag{A.1}$$

First notice that the argument in (A.1) is positive definite as $\mathbf{V}_{\mathrm{d}}(x)$ is always positive definite. Taking the time derivative of Eq. (A.1)

$$\dot{U}(t) = \int_0^L \widetilde{\mathbf{K}}(x,t)^{\mathrm{T}}\mathbf{V}_{\mathrm{d}}(x)\frac{\partial\widetilde{\mathbf{K}}(x,t)}{\partial t}\,\mathrm{d}x.$$

Using Eq. (6)

$$\begin{aligned}\dot{U}(t) = &-\int_0^L \widetilde{\mathbf{K}}(x,t)^{\mathrm{T}}\mathbf{V}_{\mathrm{d}}(x)\frac{\partial}{\partial x}\{\mathbf{V}_{\mathrm{d}}(x)\widetilde{\mathbf{K}}(x,t)\}\,\mathrm{d}x + \int_0^L \widetilde{\mathbf{K}}(x,t)^{\mathrm{T}}\mathbf{V}_{\mathrm{d}}(x)\frac{\partial}{\partial x}\{\mathbf{V}_{\mathrm{f}}(x,t)\mathbf{K}(x,t)\}\,\mathrm{d}x\\ &+\int_0^L \widetilde{\mathbf{K}}(x,t)^{\mathrm{T}}\mathbf{V}_{\mathrm{d}}(x)\mathbf{N}_{\mathrm{d}}(x,t)\widetilde{\mathbf{K}}(x,t)\,\mathrm{d}x - \int_0^L \widetilde{\mathbf{K}}(x,t)^{\mathrm{T}}\mathbf{V}_{\mathrm{d}}(x)\mathbf{N}_{\mathrm{f}}(x,t)\mathbf{K}(x,t)\,\mathrm{d}x.\end{aligned} \tag{A.2}$$

The first integral in Eq. (A.2) is an exact differential and the second can be rewritten using Lebnitz's rule. Thus,

$$\dot{U}(t) = -\widetilde{\mathbf{K}}(x,t)^{\mathrm{T}}\mathbf{V}_{\mathrm{d}}(x)\mathbf{V}_{\mathrm{d}}(x)\widetilde{\mathbf{K}}(x,t)\Big|_0^L - \int_0^L \frac{\partial}{\partial x}\left\{\widetilde{\mathbf{K}}(x,t)^{\mathrm{T}}\mathbf{V}_{\mathrm{d}}(x)\right\}\mathbf{V}_{\mathrm{f}}(x,t)\mathbf{K}(x,t)\,\mathrm{d}x + \widetilde{\mathbf{K}}(x,t)^{\mathrm{T}}\mathbf{V}_{\mathrm{d}}(x)\mathbf{V}_{\mathrm{f}}(x,t)\mathbf{K}(x,t)\Big|_0^L + \int_0^L \widetilde{\mathbf{K}}(x,t)^{\mathrm{T}}\mathbf{V}_{\mathrm{d}}(x)\mathbf{N}_{\mathrm{d}}(x,t)\widetilde{\mathbf{K}}(x,t)\,\mathrm{d}x - \int_0^L \widetilde{\mathbf{K}}(x,t)^{\mathrm{T}}\mathbf{V}_{\mathrm{d}}(x)\mathbf{N}_{\mathrm{f}}(x,t)\mathbf{K}(x,t)\,\mathrm{d}x. \tag{A.3}$$

Recall that, by theorem assumption, $\widetilde{\mathbf{K}}(0,t) = 0$. Select matrices $\mathbf{V}_{\mathrm{f}}(x,t)$ and $\mathbf{N}_{\mathrm{f}}(x,t)$ according to Eqs. (7) and (8). Then Eq. (A.3) becomes

$$\dot{U}(t) \leqslant \int_0^L \widetilde{\mathbf{K}}(x,t)^{\mathrm{T}}\mathbf{V}_{\mathrm{d}}(x)\mathbf{N}_{\mathrm{d}}(x,t)\widetilde{\mathbf{K}}(x,t)\,\mathrm{d}x. \tag{A.4}$$

Assumption 1 establishes that $\mathbf{N}_{\mathrm{d}}(x,t)$ has a tri-diagonal structure and requires specification of only net lane changes. Therefore, it is possible to consider separately any two pair of adjacent lanes i and j with $|i-j| = 1$ to analyze the term inside the integral in Eq. (A.4). According to this Eq. (A.4) can be rewritten as

$$\dot{U}(t) \leqslant \sum_{\substack{i=1\\|i-j|=1}}^{n} \int_0^L R_{i,j}(x,t)\,\mathrm{d}x = \sum_{\substack{i=1\\|i-j|=1}}^{n} \int_0^L -n_{\mathrm{d}_{i,j}}(x,t)\left(\widetilde{K}_i(x,t)V_{\mathrm{d}_i}(x) - \widetilde{K}_j(x,t)V_{\mathrm{d}_j}(x)\right)\widetilde{K}_i(x,t)\,\mathrm{d}x, \tag{A.5}$$

where $|i-j| = 1$ and, without loss of generality, it is assumed that $n_{\mathrm{d}_{i,j}}(x,t) > 0$ and $n_{\mathrm{d}_{j,i}}(x,t) = 0$.

There are six possible combinations for the sign of $R_{i,j}(x,t)$ in Eq. (A.5) that depend on the signs of $\widetilde{K}_i(x,t)$, $\widetilde{K}_j(x,t)$ and the sign of the argument $\left(\widetilde{K}_i(x,t)V_{\mathrm{d}_i}(x) - \widetilde{K}_j(x,t)V_{\mathrm{d}_j}(x)\right)$. These combinations are

1. If $\widetilde{K}_i(x,t) = 0$ or $\widetilde{K}_j(x,t) = 0 \Rightarrow R_{i,j}(x,t) \leqslant 0$.
2. If $\operatorname{sign}(\widetilde{K}_i(x,t)) \neq \operatorname{sign}(\widetilde{K}_j(x,t)) \Rightarrow R_{i,j}(x,t) \leqslant 0$.
3. If $\widetilde{K}_i(x,t), \widetilde{K}_j(x,t) > 0$ and $\widetilde{K}_i(x,t)V_{\mathrm{d}_i}(x) > \widetilde{K}_j(x,t)V_{\mathrm{d}_j}(x) \Rightarrow R_{i,j}(x,t) \leqslant 0$.
4. If $\widetilde{K}_i(x,t), \widetilde{K}_j(x,t) > 0$ and $\widetilde{K}_i(x,t)V_{\mathrm{d}_i}(x) < \widetilde{K}_j(x,t)V_{\mathrm{d}_j}(x) \Rightarrow R_{i,j}(x,t) \geqslant 0$.
5. If $\widetilde{K}_i(x,t), \widetilde{K}_j(x,t) < 0$ and $\widetilde{K}_i(x,t)V_{\mathrm{d}_i}(x) < \widetilde{K}_j(x,t)V_{\mathrm{d}_j}(x) \Rightarrow R_{i,j}(x,t) \leqslant 0$.
6. If $\widetilde{K}_i(x,t), \widetilde{K}_j(x,t) < 0$ and $\widetilde{K}_i(x,t)V_{\mathrm{d}_i}(x) > \widetilde{K}_j(x,t)V_{\mathrm{d}_j}(x) \Rightarrow R_{i,j}(x,t) \geqslant 0$.

Notice that $\dot{U}(t) \leqslant 0$ for all cases with the exception of items 4 and 6 in the previous list. [2] To show $\mathscr{L}_2$ stability for $\widetilde{\mathbf{K}}(\cdot,t) = 0$ for those two cases define $L_{4_{i,j}}$ and $L_{6_{i,j}}$ to be the union of all the segments of the highway length $[0,L]$ where conditions 4 and 6 hold, respectively for lanes i and j, $|i-j| = 1$. And let L_4 and L_6 be the collection of all $L_{4_{i,j}}$ and $L_{6_{i,j}}$, respectively.

Case 4, $\widetilde{K}_i(x,t), \widetilde{K}_j(x,t) > 0$ and $\widetilde{K}_i(x,t)V_{\mathrm{d}_i}(x) < \widetilde{K}_j(x,t)V_{\mathrm{d}_j}(x)$. From Eq. (A.5) evaluated for segments $L_{4_{i,j}}$

[2] The trivial case when $n_{\mathrm{d}_{i,j}}(x,t) = n_{\mathrm{d}_{j,i}}(x,t) = 0$ is not considered in the analysis. It does not present any problem from the stability point of view.

$$\dot{U}(t)|_{L_4} \leqslant -\sum_{\substack{i=1\\|i-j|=1}}^{n} \int_{L4_{i,j}} n_{\mathrm{d}_{i,j}}(x,t)\left(\widetilde{K}_i(x,t)V_{\mathrm{d}_i}(x) - \widetilde{K}_j(x,t)V_{\mathrm{d}_j}(x)\right)\widetilde{K}_i(x,t)\,\mathrm{d}x$$

$$= \sum_{\substack{i=1\\|i-j|=1}}^{n}\left\{ -\int_{L4_{i,j}} \widetilde{K}_i(x,t)^2 V_{\mathrm{d}_i}(x) n_{\mathrm{d}_{i,j}}(x,t)\,\mathrm{d}x + \int_{L4_{i,j}} \widetilde{K}_i(x,t)\widetilde{K}_j(x,t)V_{\mathrm{d}_j}(x)n_{\mathrm{d}_{i,j}}(x,t)\,\mathrm{d}x\right\}$$

$$\leqslant -2\underline{n}_{\mathrm{d}}(t)U(t)|_{L_4} + \sum_{\substack{i=1\\|i-j|=1}}^{n}\int_{L_4} \widetilde{K}_j(x,t)\left(\widetilde{K}_i(x,t)+\widetilde{K}_j(x,t)\right)V_{\mathrm{d}_j}(x)n_{\mathrm{d}_{i,j}}(x,t)\,\mathrm{d}x, \tag{A.6}$$

where

$$\underline{n}_{\mathrm{d}}(t) = \inf_{\substack{x\in L4_{i,j}\\ i,|i-j|=1}} \{n_{\mathrm{d}_{i,j}}(x,t)\}.$$

The desired density is always prescribed to be bounded, i.e., $0 \leqslant \alpha K_{\mathrm{d}_i}(x,t)$, $\alpha K_{\mathrm{d}_j}(x,t) < M < \infty$. As $\widetilde{K}_i(x,t)$, $\widetilde{K}_j(x,t) > 0$, this implies that there exists M such that $\widetilde{K}_i(x,t) < M\ \forall i$.

Define

$$\overline{V}_{\mathrm{d}_j} = \sup_{\substack{x\in L4_{i,j}\\ i,|i-j|=1}} \{V_{\mathrm{d}_j}(x)\},$$

$$\bar{n}_{\mathrm{d}_{i,j}}(t) = \sup_{\substack{x\in L4_{i,j}\\ i,|i-j|=1}} \{n_{\mathrm{d}_{i,j}}(x,t)\}.$$

Then

$$\dot{U}(t)|_{L_4} \leqslant -2\underline{n}_{\mathrm{d}}(t)U(t)|_{L_4} + \sum_{\substack{i=1\\|i-j|=1}}^{n} 2M^2\overline{V}_{\mathrm{d}_j}\bar{n}_{\mathrm{d}_{i,j}}(t)\left(\int_{L4_{i,j}}\mathrm{d}x\right) \leqslant -2\underline{n}_{\mathrm{d}_{i,j}}(t)U_{L_4}(t) + \beta, \tag{A.7}$$

where

$$\beta = 2M^2\sum_{\substack{i=1\\|i-j|=1}}^{n}\overline{V}_{\mathrm{d}_j}\bar{n}_{\mathrm{d}_{i,j}}(t)\left(\int_{L4_{i,j}}\mathrm{d}x\right).$$

Eq. (A.7) implies that $U(t)|_{L_4}$ can at most grow to the point where

$$U(t)|_{L_4} = \frac{\beta}{2\underline{n}_{\mathrm{d}}(t)}$$

and therefore $\mathscr{L}_2$ stability for $\widetilde{\mathbf{K}}(\cdot,t) = 0$ follows for this case.

Case 6, $\widetilde{K}_i(x,t), \widetilde{K}_j(x,t) < 0$ and $\widetilde{K}_i(x,t)V_{\mathrm{d}_i}(x) > \widetilde{K}_j(x,t)V_{\mathrm{d}_j}(x)$.

When there is desired lane change, the lanes in a highway can be classified in one of three classes:

1. Lanes that lose vehicles to both adjacent lanes.
2. Lanes that lose vehicles to one adjacent lane and gain vehicles from the other adjacent lane.
3. Lanes that only gain vehicles from both adjacent lanes.

Assume that lane i belongs to the first class, then the time derivative of the ith component in Eq. (A.5) is

$$\dot{U}_i(t)|_{L6_{i,j}} \leqslant -\sum_{|i-j|=1} \int_{L6_{i,j}} n_{\mathrm{d}_{i,j}}(x,t)\widetilde{K}_i(x,t)^2 V_{\mathrm{d}_i}(x)\,\mathrm{d}x \leqslant -4\underline{n}_{\mathrm{d}_i}(t)U_i(t)|_{L6_{i,j}}, \tag{A.8}$$

where

$$\underline{n}_{\mathrm{d}_i}(t) = \inf_{\substack{x\in L6_{i,j}\\ i,|i-j|=1}} \{n_{\mathrm{d}_{i,j}}(x,t)\}.$$

Eq. (A.8) implies that

$$\lim_{t\to\infty} \widetilde{K}_i(x,t)|_{L6_{i,j}} = 0 \tag{A.9}$$

for all lanes that do not receive vehicles because of lane change.

Now assume that lane i belongs to the second class, then the time derivative of the ith component in Eq. (A.5) is

$$\dot{U}_i(t)|_{L6_{i,j}} \leqslant -\int_{L6_{i,j}} n_{\mathrm{d}_{i,j}}(x,t)\widetilde{K}_i(x,t)^2 V_{\mathrm{d}_i}(x) + \int_{L6_{i,k}} n_{\mathrm{d}_{k,i}}(x,t)\widetilde{K}_i(x,t)\widetilde{K}_k(x,t)V_{\mathrm{d}_i}(x)\,\mathrm{d}x, \tag{A.10}$$

where lane j is the lane to which vehicles are send to and lane k is the lane from which vehicles are received from. Lanes in class 2 can form groups of adjacent lanes, however, this group must have a class 1 lane in one side and a class 3 lane in the other. Therefore, it is possible to assume, without loss of generality, that in Eq. (A.10) lane k belongs to the class 1. Given $\varepsilon > 0$ and using Eq. (A.9) it follows that after a long enough time t_0, $|\widetilde{K}_k(x,t)| < \varepsilon$ and therefore

$$\dot{U}_i(t)|_{L6_{i,j}} \leqslant -2\underline{n}_{\mathrm{d}_i}(t)U_i(t)|_{L6_{i,j}} + M\varepsilon U_j(t)^{1/2}|_{L6_{i,k}}, \tag{A.11}$$

where

$$M = \sup_{x\in L6_{i,k}} \{V_{\mathrm{d}_i}^{1/2}(x)\} \sup_{x\in L6_{i,k}} \{n_{\mathrm{d}_{k,i}}(x,t)\} \left(\int_{L6_{i,k}} \mathrm{d}x\right)^{1/2}.$$

Using

$$\frac{\mathrm{d}}{\mathrm{d}t}\left(U(t)^{1/2}\right) = \frac{1}{2}U(t)^{-1/2}\dot{U}(t), \tag{A.12}$$

it follows that

$$\frac{\mathrm{d}}{\mathrm{d}t}\left(U_i(t)^{1/2}|_{L6_{i,k}}\right) \leqslant -\underline{n}_{\mathrm{d}_{i,j}}(t)U_i(t)^{1/2}|_{L6_{i,k}} + M\varepsilon. \tag{A.13}$$

As ε can be made arbitrarily small, Eq. (A.13) implies that

$$\lim_{t\to\infty} \widetilde{K}_i(x,t)|_{L6_{i,k}} = 0. \tag{A.14}$$

Once Eq. (A.14) is applied to the first lane in a group of adjacent class 2 lanes, the argument in Eqs. (A.11)–(A.13) can be repeated for all the lanes in that group and for all groups of class 2 lanes, therefore Eq. (A.14) holds for all lanes in class 2.

Finally, if lane i belongs to the third class, then the time derivative of the ith component in Eq. (A.5) is

$$\dot{U}_i(t)|_{L_{6_{i,j}}} \leqslant \sum_{|i-j|=1} \int_{L_{6_{i,j}}} n_{\mathrm{d}_{j,i}}(x,t)\widetilde{K}_i(x,t)\widetilde{K}_j(x,t)V_{\mathrm{d}_i}(x)\,\mathrm{d}x. \tag{A.15}$$

Eqs. (A.9) and (A.14) show that given $\varepsilon > 0$, after a long enough time t_1, $|\widetilde{K}_j(x,t)| < \varepsilon$ for the adjacent lanes to those in class 3, therefore using again Eq. (A.12)

$$\lim_{t\to\infty} \frac{\mathrm{d}}{\mathrm{d}t}\left(U_i(t)^{1/2}|_{L_{6_{i,j}}}\right) = 0. \tag{A.16}$$

Eq. (A.16) implies, in turn

$$|\widetilde{K}_i(x,t)| < M < \infty \quad \forall t > t_1, \;\; x \in L_{6_{i,j}} \tag{A.17}$$

and therefore the density error in all class 3 lanes is bounded. Eqs. (A.9), (A.14) and (A.17) imply that $|\widetilde{\mathbf{K}}(x,t)|$ is also bounded and therefore, $\mathscr{L}_2$ stability for $\widetilde{\mathbf{K}}(\cdot,t) = 0$ hold also for case 6.

Once the $\mathscr{L}_2$ stability for $\widetilde{\mathbf{K}}(\cdot,t) = 0$ is proved, it is possible to analyze the influence of the terms in Eq. (A.3) in the equilibrium of the dynamics of the density error in Eq. (6).

Consider first the case when $\mathbf{V}(0,t)\mathbf{K}(0,t) = \alpha\mathbf{V}_{\mathrm{d}}(0)\mathbf{K}_{\mathrm{d}}(0,t)$. This implies $\widetilde{\mathbf{K}}(0,t) = \mathbf{0}$. In Eq. (A.3), the first boundary term is negative and the two feedback terms (the second and fifth) are negative semidefinite. The third term vanish because $\gamma(0,t) = \gamma_i(L,t) = 0$. As time passes the sign of $R_{i,j}(x,t)$ for all $x \in [0,l]$ in Eq. (A.5) will fall in case 1. Therefore $\dot{U}(t)$ becomes negative definite and Lyapunov theory guarantees that $\widetilde{\mathbf{K}}(0,t) = \mathbf{0}$ is an stable asymptotic equilibrium of because of Eq. (6).

Consider now the case when $\mathbf{V}(0,t)\mathbf{K}(0,t) \neq \alpha\mathbf{V}_{\mathrm{d}}(0)\mathbf{K}_{\mathrm{d}}(0,t)$. In this situation $U(t) = 0$ is not a possible value. Analyzing again Eq. (A.3) to look for a minimum of $U(t)$ it follows that $\dot{U}(t) = 0$ will occur when all the terms in this equation vanish. This occurs precisely in the equilibrium in Eqs. (10) and (11). In particular notice that the i,j elements inside the integrals of the fourth and fifth terms in Eq. (A.3) are

$$-n_{\mathrm{d}_{i,j}}(x,t)\left(\widetilde{K}_i(x,t)V_{\mathrm{d}_i}(x) - \widetilde{K}_j(x,t)V_{\mathrm{d}_j}(x)\right)\widetilde{K}_i(x,t) \tag{A.18}$$

and

$$-\zeta_{i,j}(x,t)\left(\widetilde{K}_i(x,t)V_{\mathrm{d}_i}(x) - \widetilde{K}_j(x,t)V_{\mathrm{d}_j}(x)\right)^2 K_j(x,t) \tag{A.19}$$

respectively. These two terms vanish when

$$\widetilde{K}_i(x,t)V_{\mathrm{d}_i}(x) = \widetilde{K}_j(x,t)V_{\mathrm{d}_j}(x). \tag{A.20}$$

Note that when the inlet flow equals $\mathbf{V}(0,t)\mathbf{K}(0,t) = \beta\mathbf{V}_{\mathrm{d}}(0,t)\mathbf{K}_{\mathrm{d}}(0,t)$, with $\beta \neq \alpha$, the boundary term in Eq. (A.3)

$$\mathbf{K}_{\mathrm{d}}(0,t)^{\mathrm{T}}\mathbf{V}_{\mathrm{d}}(0)\mathbf{V}_{\mathrm{d}}(0)\mathbf{K}_{\mathrm{d}}(0,t) \neq 0.$$

As time passes, the feedback terms in the control laws will zero the gradient of the weighted density error and therefore this term will be compensated by the other boundary term

$$\mathbf{K}_{\mathrm{d}}(L,t)^{\mathrm{T}}\mathbf{V}_{\mathrm{d}}(L)\mathbf{V}_{\mathrm{d}}(L)\mathbf{K}_{\mathrm{d}}(L,t)$$

in such a way that

$$\mathbf{K}_{\mathrm{d}}(0,t)^{\mathrm{T}}\mathbf{V}_{\mathrm{d}}(0)\mathbf{V}_{\mathrm{d}}(0)\mathbf{K}_{\mathrm{d}}(0,t) - \mathbf{K}_{\mathrm{d}}(L,t)^{\mathrm{T}}\mathbf{V}_{\mathrm{d}}(L)\mathbf{V}_{\mathrm{d}}(L)\mathbf{K}_{\mathrm{d}}(L,t) = 0. \qquad \square$$

Remark

1. Eqs. (9)–(11) can be interpreted in terms of the performance of the controller. Eq. (9) is the most desired case. The traffic situation is such that it is possible to achieve perfect density tracking. When this is not possible, because the real number of vehicles in the highway section does not coincide with the desired number, then the controller can only try to balance the weighted density error, as indicated in Eqs. (10) and (11).
2. Theorem 1 allows to lane change even when the adjacent lanes have different desired velocities. This was not the case in Li et al. (1995) and Li et al. (1997a,b), where a connectivity constraint was necessary. This connectivity constraint was introduced to allow a diagonal structure in a matrix $\mathbf{A}(x)$ that performed a change of coordinates. Commutation of the product of diagonal matrices was used to guarantee a diagonal structure in the matrix $\mathbf{P}(x) = \mathbf{A}(x)\Sigma(x)\mathbf{A}^{-1}(x)$, where $\Sigma(x)$ was a diagonal matrix expressing the connectivity constraint. In contrast, in Theorem 1 the structure of the matrix $\mathbf{N}_{\mathrm{f}}(x,t)$ is exploited to derive the stability of the control laws.

Appendix B. Proof of Theorem 2

Proof. Choose the following Lyapunov function candidate

$$U_{\omega}(t) = \frac{1}{2}\int_0^L \widetilde{\mathbf{K}}_{\omega}(x,t)^{\mathrm{T}}\mathbf{V}_{\omega_{\mathrm{d}}}(x)\widetilde{\mathbf{K}}_{\omega}(x,t)\,\mathrm{d}x. \tag{B.1}$$

Taking the time derivative of Eq. (B.1)

$$\dot{U}_{\omega}(t) = \int_0^L \widetilde{\mathbf{K}}_{\omega}(x,t)\mathbf{V}_{\omega_{\mathrm{d}}}(x)\frac{\partial\widetilde{\mathbf{K}}_{\omega}(x,t)}{\partial t}\,\mathrm{d}x.$$

Using Eq. (19)

$$\begin{aligned}\dot{U}_{\omega}(t) = &-\int_0^L \widetilde{\mathbf{K}}_{\omega}(x,t)^{\mathrm{T}}\mathbf{V}_{\omega_{\mathrm{d}}}(x)\frac{\partial}{\partial x}\{\mathbf{V}_{\omega_{\mathrm{d}}}(x)\widetilde{\mathbf{K}}_{\omega}(x,t)\}\,\mathrm{d}x + \int_0^L \widetilde{\mathbf{K}}_{\omega}(x,t)^{\mathrm{T}}\mathbf{V}_{\omega_{\mathrm{d}}}(x)\\ &\times\frac{\partial}{\partial x}\{\mathbf{V}_{\omega_{\mathrm{f}}}(x,t)\mathbf{K}_{\omega}(x,t)\}\,\mathrm{d}x + \int_0^L \widetilde{\mathbf{K}}_{\omega}(x,t)^{\mathrm{T}}\mathbf{V}_{\omega_{\mathrm{d}}}(x)\mathbf{N}_{\omega_{\mathrm{d}}}(x,t)\widetilde{\mathbf{K}}_{\omega}(x,t)\,\mathrm{d}x\\ &-\int_0^L \widetilde{\mathbf{K}}_{\omega}(x,t)^{\mathrm{T}}\mathbf{V}_{\omega_{\mathrm{d}}}(x)\mathbf{N}_{\omega_{\mathrm{f}}}(x,t)\mathbf{K}_{\omega}(x,t)\,\mathrm{d}x.\end{aligned} \tag{B.2}$$

The first integral in Eq. (B.2) is an exact differential and the second can be rewritten using Lebnitz's rule. Thus,

$$\dot{U}_\omega(t) = -\widetilde{\mathbf{K}}_\omega(x,t)^{\mathrm{T}}\mathbf{V}_{\omega_{\mathrm{d}}}(x)\mathbf{V}_{\omega_{\mathrm{d}}}(x)\widetilde{\mathbf{K}}_\omega(x,t)\Big|_0^L - \int_0^L \frac{\partial}{\partial x}\left\{\widetilde{\mathbf{K}}_\omega(x,t)^{\mathrm{T}}\mathbf{V}_{\omega_{\mathrm{d}}}(x)\right\}\mathbf{V}_{\omega_{\mathrm{f}}}(x,t)(x,t)\,\mathrm{d}x$$
$$+ \widetilde{\mathbf{K}}_\omega(x,t)^{\mathrm{T}}\mathbf{V}_{\omega_{\mathrm{d}}}(x)\mathbf{V}_{\omega_{\mathrm{f}}}(x,t)\mathbf{K}_\omega(x,t)\Big|_0^L + \int_0^L \widetilde{\mathbf{K}}_\omega(x,t)^{\mathrm{T}}\mathbf{V}_{\omega_{\mathrm{d}}}(x)\mathbf{N}_{\omega_{\mathrm{d}}}(x,t)\widetilde{\mathbf{K}}_\omega(x,t)\,\mathrm{d}x$$
$$- \int_0^L \widetilde{\mathbf{K}}_\omega(x,t)^{\mathrm{T}}\mathbf{V}_{\omega_{\mathrm{d}}}(x)\mathbf{N}_{\omega_{\mathrm{f}}}(x,t)\mathbf{K}_\omega(x,t)\,\mathrm{d}x. \tag{B.3}$$

Use the fact that, by assumption, $\widetilde{\mathbf{K}}_\omega(0,t) = 0$, and select matrices $\mathbf{V}_{\omega_{\mathrm{f}}}(x,t)$ and $\mathbf{N}_{\omega_{\mathrm{f}}}(x,t)$ according to Eqs. (22) and (23). Then proceed as in the proof of Theorem 1 to conclude on the $\mathscr{L}_2$ stability for $\widetilde{\mathbf{K}}_\omega(\cdot,t) = 0$ and the points of equilibria. □

Remark. Theorem 2 also allows lane change even when the adjacent lanes have different desired velocity. The implementation of the link layer control law in Theorem 2 can be distributed, as only information from neighbor positions is required.

References

Alvarez, L., Horowitz, R., Chao, S., Gomes, G., 1998. Optimal desired traffic flow patterns for Automated Highway Systems. In: Proceedings of the American Control Conference.

Alvarez, L., Horowitz, R., Li, P., 1999. Traffic Flow control in automated highways systems. Control Engineering Practice 7 (9), 1071–1078.

Broucke, M., Varaiya, P., 1996. A theory of traffic flow in automated highway system. Transportation Research, Part C: Emerging Technologies 4 (4), 181–210.

Broucke, M., Varaiya, P., Kourjankski, M., Khorramabadi, D., 1996, May. Smartcap User's Guide. Technical report, Department of Electrical Engineering and Computer Science, University of California, Berkeley, California.

Chien, C.C., Zhang, Y., Stotsky, A., 1993, December. Traffic density tracker for automated highway systems. In: Proceedings of the 33rd IEEE CDC.

Eskafi, F., Khorramabadi, D., Varaiya, P., 1992. Smartpath: an automated highway system simulator. Technical Report PATH Memorandum 92-3, Institute of Transportation Studies, University of California, Berkeley.

Godbole, D.N., Lygeros, J., 1994. Longitudinal control of the lead car of a platoon. IEEE Transactions on Vehicular Technology 43 (4), 1125–1135, Also in Proceedings of the 1994 ACC.

Hsu, A., Eskafi, F., Sachs, S., Varaiya, P., 1991. The design of platoon maneuver protocols for IVHS. Technical Report, UCB-ITS-PRR-91-6, University of California, Berkeley.

Karaaslan, U., Varaiya, P. Walrand, J., 1990. Two proposals to improve freeway traffic flow. Technical report, UCB-ITS-PRR-90-6, University of California, Berkeley.

Li, P., Horowitz, R., Alvarez, L., Frankel, J., Roberston, A., 1995, November. An AVHS link layer controller for traffic flow stabilization. Technical report, UCB-PATH TECH NOTE 95-7, Institute of Transportation Studies, PATH, University of California, Berkeley, CA 94720.

Li, P., Alvarez, L., Horowitz, R., 1997a. AVHS safe control laws for platoon leaders. IEEE Transactions on Control Systems Technology 5 (6), 614–628.

Li, P., Horowitz, R., Alvarez, L., Frankel, J., Roberston, A., 1997b. An AHS link layer controller for traffic flow stabilization. Transportation Research, Part C: Emerging Technologies 5 (1), 11–37.

Papageorgiou, M., Blosseville, J.M., Hadi-Salem, H., 1990. Modelling and real-time control of traffic flow on the southern part of Boulevard Peripherique in Paris: Part i: modelling and part ii: coordinated on-ramp metering. Transportation Research, Part A 24 (5), 345–370.

Rao, B., Varaiya, P., 1994. Roadside intelligence for flow control in an intelligent vehicle and highway system. Transportation Research, Part C 2 (1), 49–72.

Swaroop, D., Chien, C., Hedrick, J., Ioannou, P., 1994. Comparison of spacing and headway control laws for automatically controlled vehicles. Vehicle System Dynamics 8, 597–625.

Varaiya, P., 1993. Smart cars on smart roads: problems of control. IEEE Transactions on Automatic Control AC 38 (2), 195–207.

Varaiya, P., Shladover, S.E., 1991. Sketch of an IVHS systems architecture. Technical Report UCB-ITS-PRR-91-3, Institute of Transportation Studies, University of California, Berkeley.